



HAL
open science

Numerical study of the aero-thermal performance for different scenarios of a refrigerated truck using URANS

M.A. Ben Taher, M. Mahdaoui, Tarik Kousksou, Y. Zeraouli, M. Ahachad

► To cite this version:

M.A. Ben Taher, M. Mahdaoui, Tarik Kousksou, Y. Zeraouli, M. Ahachad. Numerical study of the aero-thermal performance for different scenarios of a refrigerated truck using URANS. *Journal of Cleaner Production*, 2021, 320, pp.128775. 10.1016/j.jclepro.2021.128775 . hal-04482363

HAL Id: hal-04482363

<https://univ-pau.hal.science/hal-04482363>

Submitted on 22 Jul 2024

HAL is a multi-disciplinary open access archive for the deposit and dissemination of scientific research documents, whether they are published or not. The documents may come from teaching and research institutions in France or abroad, or from public or private research centers.

L'archive ouverte pluridisciplinaire **HAL**, est destinée au dépôt et à la diffusion de documents scientifiques de niveau recherche, publiés ou non, émanant des établissements d'enseignement et de recherche français ou étrangers, des laboratoires publics ou privés.



Distributed under a Creative Commons Attribution - NonCommercial 4.0 International License

Numerical study of the aero-thermal performance for different scenarios of a refrigerated truck using URANS

M. A. Ben Taher ^{1,2}, M. Mahdaoui ², T. Kousksou ¹, Y. Zeraouli ¹, M. Ahachad ²

¹ Université de Pau et des Pays de l'Adour, E2S UPPA, SIAME, Pau, 64000, France.

² Equipe de Recherche en Transferts Thermiques & Énergétique, Faculté des Sciences et Techniques de Tanger, Université Abdelmalek Essaadi, Tetouan, Maroc.

Abstract:

The cold chain represents a sensitive element that directly affects the food security of our society. Refrigerated truck transport directly affects the quality and shelf life of perishable products according to their appropriate temperature ranges, which are key elements of the chain. In this context, it is important to examine the cooling mechanism to improve and optimize the energy efficiency inside the container. However, this study was conducted to gain knowledge of aerothermal behavior and to understand the flow mechanisms in various three-dimensional configurations of trucks using URANS. The numerical results obtained provide a good qualitative agreement with the experimental data. Furthermore, this study reveals that an air curtain can be employed to optimize the energy consumption and cooling time when opening the truck door, considering different loading scenarios (empty, partially truckload, and almost fully truckload). While the use of this device could lead to savings up to 25.3% of the cooling energy consumption.

Keywords:

Food cold chain; energy consumption; refrigerated truck; air curtain; forced convection; CFD.

Nomenclature

List of symbols

h	convection coefficient ($\text{W m}^{-2} \text{K}^{-1}$)
Q	energy (J)
g	gravitational acceleration (m s^{-2})
K	heat transfer coefficient ($\text{W m}^{-2} \text{K}^{-1}$)
n	normal vector
C _p	specific heat capacity ($\text{J kg}^{-1} \text{K}^{-1}$)
T	temperature (K)
t	time (s)
I	turbulence intensity (%)
k	turbulent kinetic energy ($\text{m}^2 \text{s}^{-2}$)
u	velocity (m s^{-1})

Subscripts

c	curtain
f	fluid
g	goods
r	recovery
w	wall

Greek Letters

η	efficiency (%)
ρ	density (kg m^{-3})
μ	dynamic viscosity (Pa s)
λ	heat conductivity ($\text{W m}^{-1} \text{K}^{-1}$)
μ_T	turbulent viscosity (Pa s)
ε	turbulence dissipation rate ($\text{m}^2 \text{s}^{-3}$)
σ	shear stress ($\text{kg m}^{-1} \text{s}^{-2}$)
ω	specific turbulence dissipation rate (s^{-1})

Acronyms

CFD	computational fluid dynamic
FR	filled ratio
GHG	greenhouse gas
URANS	unsteady reynolds averaged navier stokes
SST	shear stress transport

1. Introduction

The refrigerated transport of perishable products has attracted a lot of attention in the last century. However, the sustainable development of these types of transport has not yet fully satisfied the basic rules of the cold chain. Specifically, the cold chain market comes to \$189.92 in 2017 and will reach \$293.27B by 2023 (BIS Research, 2019). In addition, the energy consumption and environmental impact of this chain pose a global challenge (Saguy et al., 2013), as it represents 30% of total world consumption (Kayfeci et al., 2013), and nearly 1% of global GHG emissions (James and James, 2010).

According to (de Palma et al., 2011), transport and storage costs represent 96% of logistics costs. These stats clearly underline the significance of refrigerated transport on the development of the market. Besides, the container's air during deliveries must be renewed each time the door has been opened, which makes it impossible to maintain the interior temperature.

Therefore, the employment of special equipment meeting ATP (Agreement on the International Carriage of Perishable Foodstuffs) specifications for the transport of perishable goods shall be mandatory. This agreement concerns the norms of the trucks, the temperatures of the products and the norms of hygiene and security. For this reason, it is necessary to invest in modern technologies for refrigerated commercial trucks, to guarantee the quality and the safety of the foodstuffs against the temperature variations and to reduce the energy consumption and the environmental impact during transport (Ashok et al., 2017; Ben Taher et al., 2020; O'Sullivan et al., 2014; Oltersdorf, 2003; Oró et al., 2012; Saguy et al., 2013).

Furthermore, (Tanner, 2016) discussed the different modes of refrigerated transport including air, marine, rail, and road. To this end, they showed that over one million refrigerated road vehicles are used to distribute refrigerated food around the world. In the road mode of refrigerated transport, refrigerated trucks are widely used for the transport and storage of perishable goods. These trucks have the responsibility to maintain the conservation temperatures during the whole transportation period. These requirements apply regardless of the nature of the foodstuffs (Panozzo et al., 1999; Verdouw et al., 2016).

A thorough comprehension of the phenomena, associated with temperatures and airflows in refrigerated trucks, is a complex task. In various parts of the world, different experimental studies have been carried out on this phenomenon. (Moureh et al., 2009) conducted experiments on a small-scale truck model (1/3.3). In addition to the empty truck, two loaded

configurations were studied: without and with air ducts. The results of the experiment show the importance of air ducts to reduce the internal temperature of refrigerated trucks. (Merai et al., 2019a, 2019b) predict product temperatures and refrigeration capacity during transport in a trailer loaded with pork. The same authors decided to evaluate and characterize convective heat transfer coefficients (natural and forced) with and without air distribution ducts in a scaled-down trailer loaded with rail-hung carcasses. (Jara et al., 2019) provided temperature and airflow distribution using various sensors installed at different locations in a refrigerated compartment.

In parallel with experimental work, numerical simulation using CFDs is increasingly being used to study the phenomena associated with refrigerated trucks based on aerothermal models. (Moureh et al., 2002) used Fluent to predict and characterize the airflow of a model refrigerated truck. The results can clearly show the ability of Reynolds stress model to accurately predict air movement in the loaded and unloaded scenario. (Getahun et al., 2017) evaluated the $k-\omega$ SST model using ANSYS fluent to characterize airflow and heat transfers acquired. The numerical model successfully reproduced the experimental profiles inside a truck filled with goods. (Jiang et al., 2020) improved the cooling capacity by using baffles to reduce cold air flow loss and to ensure temperature uniformity inside the truck. The $k-\omega$ SST model was validated by experimental data with acceptable accuracy. (Han et al., 2019) established a 3-D CFD model to simulate the aero-thermal flows. In order to predict the velocity and temperature distribution during cooling. A good agreement was found between the measured data and the simulated model prediction using the SST $\kappa-\omega$ model. (Senguttuvan et al., 2020) have proposed various models of refrigeration system design, to provide better airflow distribution inside a truck. In this study, a design model with a typical refrigeration unit of a refrigerated truck was used as a reference model. In order to compare the air velocity distribution with other different refrigeration unit designs. Therefore, among all cases investigated, the design of the cooling system was improved for refrigerated transport.

In addition, the effect of opening-door upon delivery leads to an increase in temperature, leading to a rise consumption of fuel and production of GHGs, thus degrading refrigeration performance and food safety (Hoang et al., 2012; Xie et al., 2021). Numerous investigations have been carried out to find the most effective methods to control air infiltration. (Tso et al., 2002) studied the effect of protected and unprotected door openings. The measurements show that the average internal air temperature increases from -10°C to 8°C and 14.7°C , with and without an air curtain respectively, after opening the door. It was found that the use of an air

curtain is effective and reduces the infiltration heat load by 40% compared to without protection during transportation. (Zhang et al., 2018) examined the influence of different sizes open-doors to improve temperature stability on a refrigerated truck. The CFD results and experiments are similar, providing a feasible method for optimizing truck design. (Cong et al., 2019) explored a parametric study of an air curtain on the internal temperature of an open-door refrigerated truck. Three key curtain characteristics were evaluated such as air flow rate, nozzle width and jet angle. It was found that an effective curtain reduces the increase in indoor air temperature after opening the door. (Lafaye De Micheaux et al., 2015) have dealt with the heat load of infiltration into the truck when its rear door was opened. The CFD model was compatible with the experimental results.

Motivation of the study

In this context, it is important to examine the cooling mechanism to improve and optimize energy efficiency inside a refrigerated truck. To the authors' knowledge, no work presents a parametric, quantitative, and optimization study for an aero-thermal model of a refrigerated truck. Besides, for reliability and to reflect a realistic situation, a model validation was carried out showing a good agreement with an experimental result recently published in the literature (Jara et al., 2019).

As a matter of fact, to complement the studies cited above, this work aims to numerically study the aerothermal behavior and to understand the flow mechanisms in three-dimensional configurations of a refrigerated truck (open-door, closed-door and semi open-door) for several loading scenarios (empty, partially truckload and almost fully truckload), using a method of combining numerical modelling and theory to achieve the following scientific objectives:

- Develop a CFD model to simulate the aerothermal behavior at different URANS unsteady turbulence models (standard k- ϵ , standard k- ω , SST k- ω) during cooling.
- Validate the predefined model with recent experimental results obtained in the literature.
- Determine the thermal energy losses through the walls of the truck.
- Evaluate the influence of Reynolds number variation on the thermal behavior of the truck to stretch the applicability of this study.
- Optimize energy consumption and cooling time when using an air curtain, considering air infiltration during door opening.
- Analyze various loading scenarios to reflect a real situation and complete this work.

- Evaluate the effect of the interaction between natural and forced convection on the cooling capacity to remove heat from the products.

This document is structured as follows. Section 2 considers the description of the system. Section 3 discusses the physical model. Section 4 outlines the results and discussion. The last section deals with the conclusion of the study.

2. System description

This paper examines a refrigerated truck with internal dimensions of about ~ 1.6 m wide (x-axis), ~ 1.7 m long (z-axis) and ~ 3 m deep (y-axis). The wall structure was composed of interior and exterior layers of steel, and the intermediate foam is a polyurethane insulation. The refrigerated compartment was equipped with cooling unit located at the top of the container.

In our case, [Fig.1] displays the four locations (inlet, outlet, door and floor) used for model validation, as well as the cross-section referenced to the aerothermal model simulation. In addition, an air curtain was installed in this truck and modeled according to the characteristics and dimensions found in the literature [Fig.2] (Brightec, 2020; Rai et al., 2019; Sirén, 2003).

Furthermore, to reflect a real situation and to complete this work, the goods cargo was modeled to be placed on a pallet of ~ 0.8 m wide (x-axis), ~ 0.8 m long (z-axis), and ~ 1.4 m deep (y-axis). Different filling rates (FR) were used for the truck loading, partially (FR = 25%), half (FR = 50%) and almost completely (FR = 75%) respectively [Fig.3].

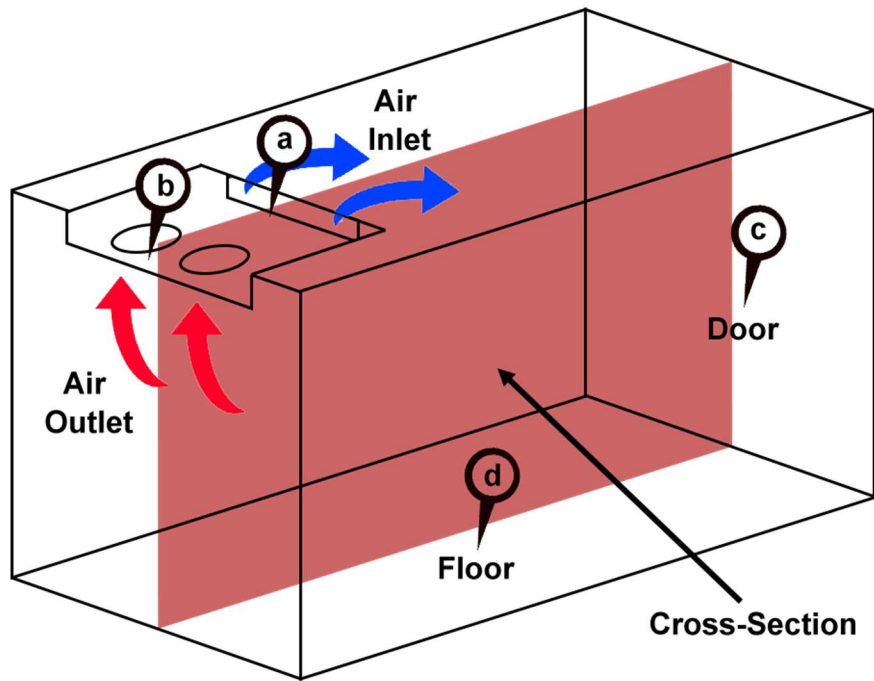


Fig. 1. 3D geometry and analysis points for the empty truck

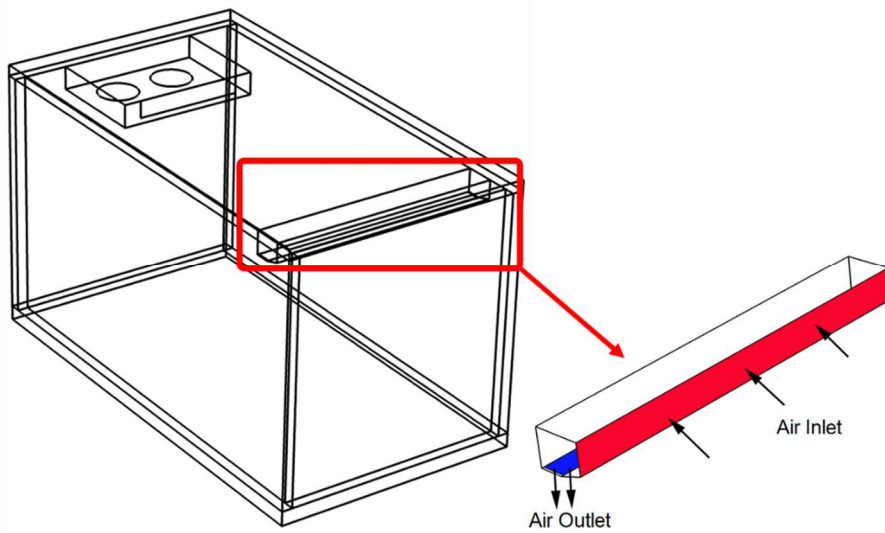


Fig. 2. 3D geometric truck model with integrated air curtain

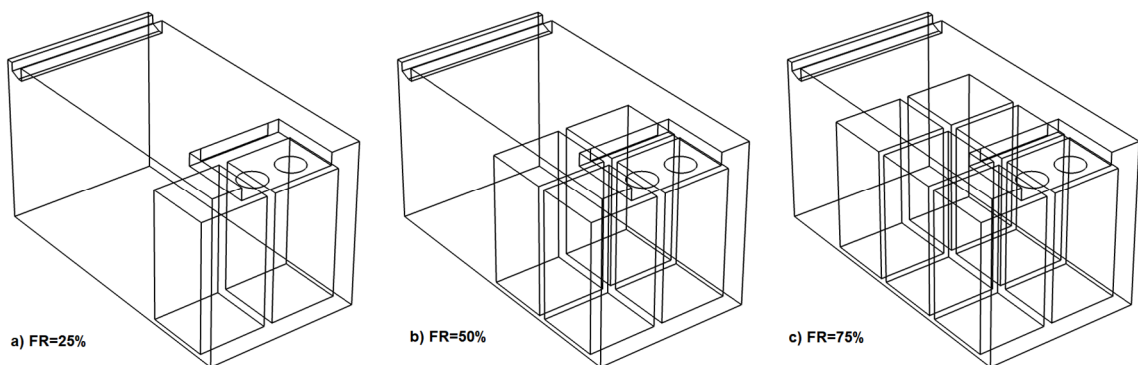


Fig. 3. Diverse internal truck loading geometries

3. Mathematical model

To simplify the calculations, this work is based on the following assumptions:

- The air inside is considered as an incompressible perfect fluid with non-constant properties.
- The boussinesq approximation and the gravity effect are considered.
- The heat exchange in the walls is applied without slip conditions.
- The air moisture interactions with energy balance were not considered.

In the context of Navier-Stokes equation analysis, the use of URANS models makes it possible to solve the phenomena of turbulence by taking into account the unsteady term. URANS models are the most widely used today in many industrial applications. Therefore, the theoretical aspects of these two-equation models are based on the Eddy-viscosity approaches (Wilcox, 2006).

3.1. Governing equations

Using the previous assumptions, the governing equations are expressed as follows:

3.1.1. For air inside the closed-door truck

The primary refrigeration unit operates when the truck door is closed. Thus, the turbulent flow and heat transfer in the refrigerated chamber are governing using Eqs. (1) - (4). Furthermore, three turbulence models were used to evaluate the aerothermal performance: $k - \omega$ SST Eq. (5) and (6) (Jones and Launder, 1972), $k - \omega$ Eq. (7) and (8) (Wilcox, 1988) and $k - \varepsilon$ Eq. (9) and (10) (Menter, 1994).

In general, turbulent viscosity is usually given by the turbulent kinetic 'k' and a variable that depends on the type of model.

$$\frac{\partial \rho_f}{\partial t} + \nabla \cdot (\rho_f u_f) = 0 \quad (1)$$

$$\rho_f \frac{\partial u_f}{\partial t} + \rho_f (u_f \cdot \nabla) u_f = \nabla \cdot [-pI + K] - \frac{2}{3} (\mu_f + \mu_T) (\nabla \cdot u_f) I - \frac{2}{3} \rho_f k I + (\rho_f - \rho_{f,0}) \vec{g} \quad (2)$$

$$K = (\mu_f + \mu_T) (\nabla u_f + (\nabla u_f)^T) \quad (3)$$

$$\rho_f C_{p,f} \frac{\partial T_f}{\partial t} + \nabla \cdot (\rho_f C_{p,f} u_f T_f - \lambda_f \vec{\nabla} T_f) = 0 \quad (4)$$

* k – ω SST model

$$\rho_f \frac{\partial k}{\partial t} + \rho_f (u_f \cdot \nabla) k = \nabla \cdot [(\mu_f + \mu_T \sigma_k^*) \nabla k] + P_k - \rho_f \beta_0^* k \omega \quad (5)$$

$$\begin{aligned} \rho_f \frac{\partial \omega}{\partial t} + \rho_f (u_f \cdot \nabla) \omega \\ = \nabla \cdot [(\mu_f + \mu_T \sigma_\omega) \nabla \omega] + \frac{\gamma}{\mu_T} \rho_f P_{SST} - \rho_f \beta_0 \omega^2 + 2(1 - f_{v1}) \frac{\sigma_\omega \rho_f}{\omega} \nabla k \cdot \nabla \omega \end{aligned} \quad (6)$$

* k – ω model

$$\rho_f \frac{\partial k}{\partial t} + \rho_f (u_f \cdot \nabla) k = \nabla \cdot [(\mu_f + \mu_T \sigma_k^*) \nabla k] + P_k - \rho_f \beta_0^* k \omega \quad (7)$$

$$\rho_f \frac{\partial \omega}{\partial t} + \rho_f (u_f \cdot \nabla) \omega = \nabla \cdot [(\mu_f + \mu_T \sigma_\omega) \nabla \omega] + \alpha \frac{\omega}{k} P_k - \rho_f \beta_0 \omega^2 \quad (8)$$

* Standard k – ε model

$$\rho_f \frac{\partial k}{\partial t} + \rho_f (u_f \cdot \nabla) k = \nabla \cdot \left[\left(\mu_f + \frac{\mu_T}{\sigma_k} \right) \nabla k \right] + P_k - \rho \varepsilon \quad (9)$$

$$\rho_f \frac{\partial \varepsilon}{\partial t} + \rho_f (u_f \cdot \nabla) \varepsilon = \nabla \cdot \left[\left(\mu_f + \frac{\mu_T}{\sigma_\varepsilon} \right) \nabla \varepsilon \right] + C_{\varepsilon 1} \frac{\varepsilon}{k} P_k - C_{\varepsilon 2} \rho_f \frac{\varepsilon^2}{k} \quad (10)$$

where T_f, u_f, ρ_f, μ_f are the temperature, velocity, density, viscosity of air, respectively, k is the turbulent kinetic, μ_T is the turbulent viscosity $\mu_T = \rho k / \omega$, ω is the specific turbulence dissipation rate, ε is the turbulence dissipation rate, I is the turbulence intensity, and $\beta_0, \beta_0^*, \sigma_k, \sigma_\omega, P_k, C_\varepsilon, f_v$ are the closure coefficients and the adjustable turbulence parameters for the different models.

3.1.2. For air inside the opened-door truck

Since the cooling unit turned off when opening the truck door, an air curtain was implemented to reduce the dissipation of cold energy. The mixed convection (natural and forced) due to the use of this device is governed by the equations Eqs. (11) - (14).

$$\rho_f \frac{\partial u_f}{\partial t} + \rho_f (u_f \cdot \nabla) u_f = \nabla \cdot [-pI + K_{op}] + (\rho_f - \rho_{f,0}) \vec{g} \quad (11)$$

$$\frac{\partial \rho_f}{\partial t} + \nabla \cdot (\rho_f u_f) = 0 \quad (12)$$

$$K_{op} = \mu_f \left(\nabla u_f + (\nabla u_f)^{T_f} \right) - \frac{2}{3} \mu_f (\nabla \cdot u_f) I \quad (13)$$

$$\rho_f C_{p,f} \frac{\partial T_f}{\partial t} + \nabla \cdot (\rho_f C_{p,f} u_f T_f - k \vec{\nabla} T_f) = 0 \quad (14)$$

3.1.3 For the chamber walls

The heat transfer in all walls is described by Eq. (15):

$$\rho_w C_{p,w} \frac{\partial T_w}{\partial t} + \nabla \cdot (\lambda_w \vec{\nabla} T_w) = 0 \quad (15)$$

where $T_w, \rho_w, C_{p,w}, \lambda_w$ are the temperature, density, specific heat, and conductivity of the wall.

3.1.4 Recovery energy and energy efficiency

The recovery energy (Q_r) and the energy efficiency (η) with and without curtains were determined based on the approaches Eq. (16) and (17), respectively.

$$Q_r = \int_v \rho_{air} C_{p,air} (T_{air} - T_{air,0}) dv_{air} + \int_{v_g} \rho_g C_{p,g} (T_g - T_{g,0}) dv_g + P_c t_c \quad (16)$$

$$\eta = 1 - \frac{Q_r}{Q_{r0}} \quad (17)$$

where (P_c) is the power of the air curtain unit in Watt, and (t_c) is its operation time, (Q_{r0}) the recovery energy through the open door without incorporating the air curtain, and ($\rho_g, C_{p,g}, T_g$) are, respectively, density, specific heat capacity and temperature of goods.

3.2 Initial and boundary conditions

The previous equations are initiated by the following conditions:

- The door closing phase has an estimated triggering time of 60 minutes with an initial truck temperature of 22.5°C.
- The door opened phase has an estimated triggering time of 15 minutes with an initial truck temperature of 0°C.

- The ventilation conditions of cooling unit are defined by a mean inlet velocity of $U_{0y}=U_0=3$ m/s, and outlet pressure at zero.
- The convection coefficient through the external face of walls was assumed to be: $h_e=3.41$ $W m^{-2} K^{-1}$.
- The air curtain is launched by an inlet velocity of $U_{0z} = 4$ m / s.
- The initial temperature of the goods is considered as $0^\circ C$.
- The thermal properties of the goods are determined at 300 ($kg m^{-3}$), 1000 ($J kg^{-1} K^{-1}$), and 0.2 ($W m^{-1} K^{-1}$) for density, specific heat capacity, and thermal conductivity, respectively (Rai et al., 2019).

Furthermore, to summarize the boundary conditions and physical parameters applied to the truck, the following (Table 1) is provided.

Table 1
Boundary conditions and physical parameters applied

Geometry Boundary	Door closed			Door Open	
	$k - \omega$	$k - \varepsilon$	$k - \omega$ SST	Curtain Off	Curtain On
Walls without door	Turbulent flow (No slip condition): $u_f \cdot n = 0$ Heat transfer (Convective exchange): $-n \cdot (-\lambda_w \nabla T_w) = h (T_{ext} - T_w)$			Laminar flow $u_f \cdot n = 0$ Heat transfer $-n \cdot (-\lambda_w \nabla T_w) = 0$	
Door				Laminar flow $[-pI + K_{op}]n = 0$ Heat transfer $T_w = T_{ext}$ if $u_f \cdot n < 0$ $(-\lambda_w \nabla T_w) = 0$ if $u_f \cdot n \geq 0$	
Cooling Air Inlet	Turbulent flow $u_f = -U_0 n$ $k = \frac{3}{2}(U_0 I_T)^2$ $\omega = \frac{k^{1/2}}{(\beta_0^*)^{1/4} L_T}$	Turbulent flow $u_f = -U_0 n$ $k = \frac{3}{2}(U_0 I_T)^2$ $\varepsilon = \frac{C_\mu^{3/4} k^{3/2}}{L_T}$	Turbulent flow $u_f = -U_0 n$ $\nabla G \cdot n = 0$ $k = \frac{3}{2}(U_0 I_T)^2$ $\omega = \frac{k^{1/2}}{(\beta_0^*)^{1/4} L_T}$	Laminar flow $u_f \cdot n = 0$ Heat transfer $-n \cdot (-\lambda_f \nabla T_f) = 0$	
	Heat transfer: Exponential fitting to experimental data (Jara et al., 2019)				

	$T_f(t) = 11.95 \exp(-0.001058 t) + 11.58 \exp(0.01036 t)$			
Cooling Air Outlet	Turbulent flow	Turbulent flow	Turbulent flow	
	$[-pI + K]n = -\widehat{p}_0 n$			
	$\nabla k \cdot n = 0$ $\nabla \omega \cdot n = 0$	$\nabla k \cdot n = 0$ $\nabla \varepsilon \cdot n = 0$	$\nabla k \cdot n = 0$ $\nabla \omega \cdot n = 0$ $\nabla G \cdot n = 0$	
	Heat transfer: $-n \cdot (-\lambda_f \nabla T_f) = 0$			
Curtain Air Inlet	--	--	--	Laminar flow $u_f = -U_0 n$ Heat transfer $T_f = T_{ext}$
Curtain Air Outlet	--	--	--	Laminar flow $u_f \cdot n = 0$ Heat transfer $-n \cdot (-\lambda_f \nabla T_f) = 0$ Laminar flow $[-pI + K_{op}]n = -\widehat{p}_0 n$ Heat transfer $-n \cdot (-\lambda_f \nabla T_f) = 0$

In this paper, the numerical model was implemented in COMSOL Multiphysics (COMSOL, 2020) to simulate the fluid dynamics and the conjugate heat transfer inside the refrigerated truck. To enhance the accuracy of this study, a mesh refinement was adopted with tetragonal elements [Fig.4]. A swept mesh was created in the walls, cooling unit, and air curtain to ensure the aerothermal performance for the CFD model. The grid size and the time step were selected after careful analysis of the autonomy of the results to these parameters [Fig.5]. The number of mesh elements was ≈ 158033 . Based on this number, a time step check leads to a value of 10-3s which was found suitable to provide accurate results. Further, the convergence is verified at each time step.

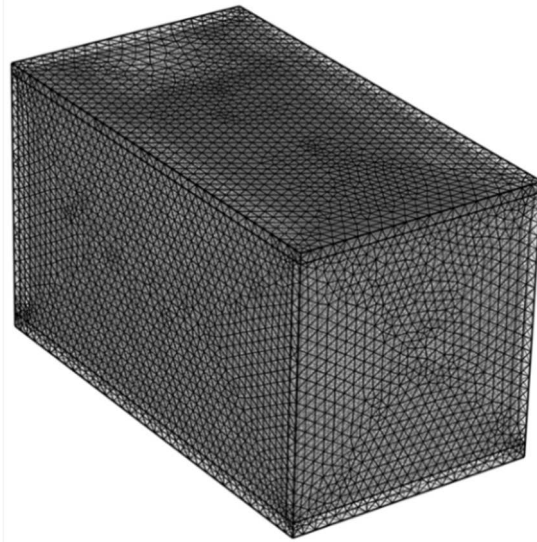


Fig. 4. Mesh defined on the truck's closed-door geometry

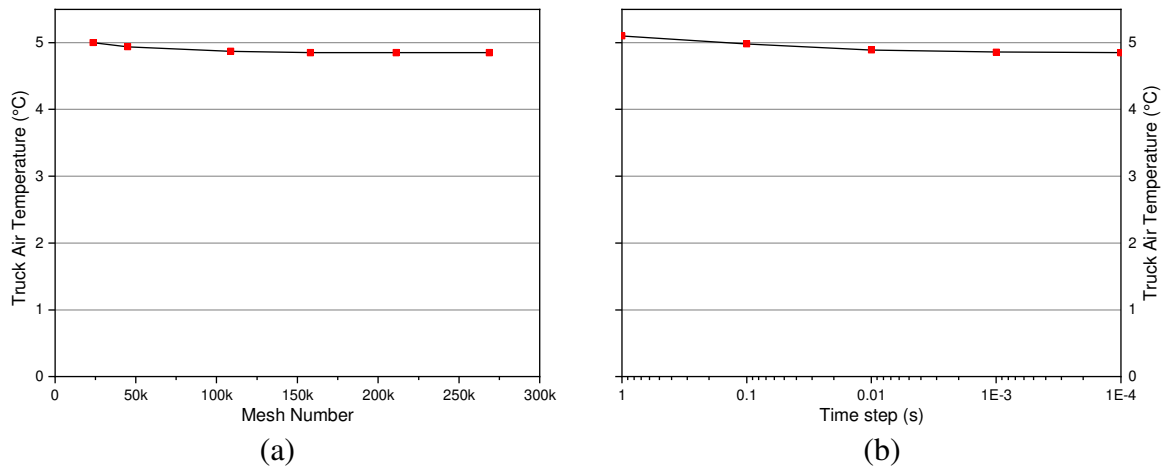


Fig. 5. Average truck air temperature variation according to (a) mesh size (b) time step

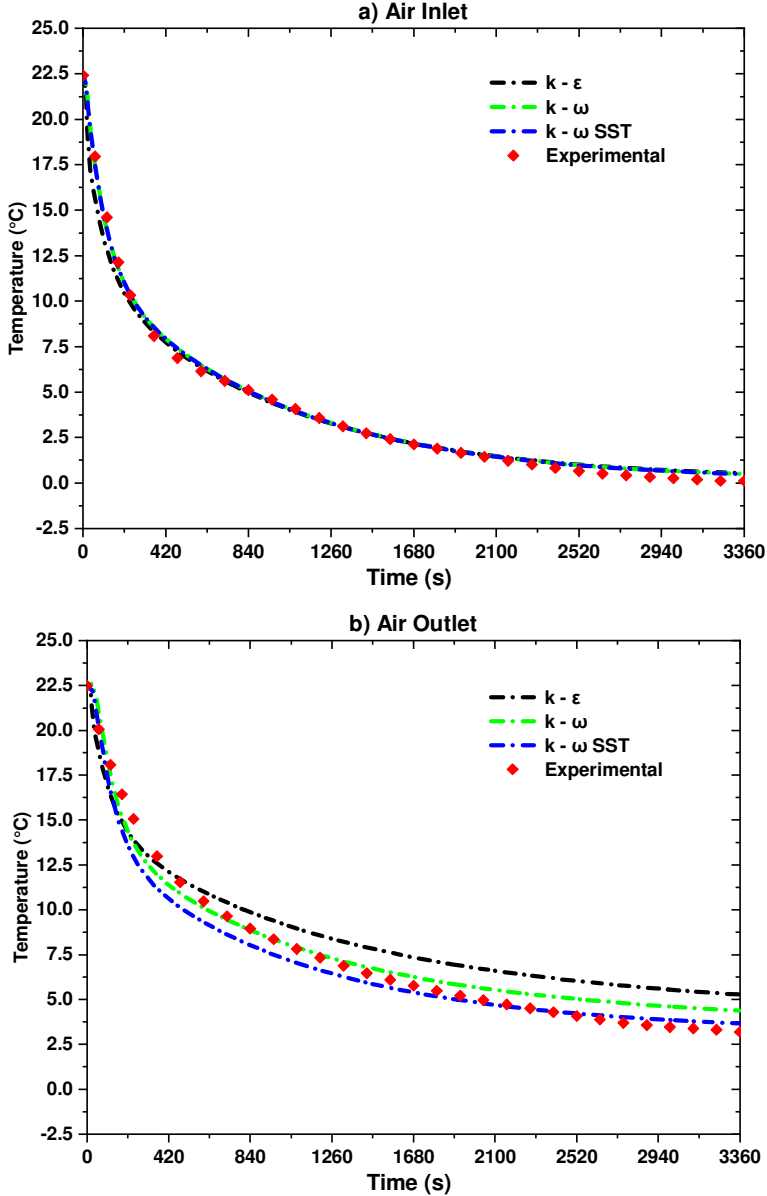
4. Result and analysis

4.1. Closed-door refrigerated truck

4.1.1. Model validation

The first part of this study aims to establish a CFD model. In order to simulate the aerothermal behavior with different models of URANS unsteady turbulence (standard κ - ω , SST κ - ω , standard κ - ϵ) in a closed-door refrigerated truck. Recent experimental work is selected for validation of this model during cooling. The results of the CFD model developed in this study present were compared with experimental results of (Jara et al., 2019).

The results obtained (internal temperature) showed that there is no significant difference between the different turbulence models and the temperatures measured in different areas of the refrigerated truck (Inlet, Outlet, Door and Floor) [Fig.6]. The difference between the simulation and experimental values can be justified by the parameters controlling the two studies and the numerical oscillations.



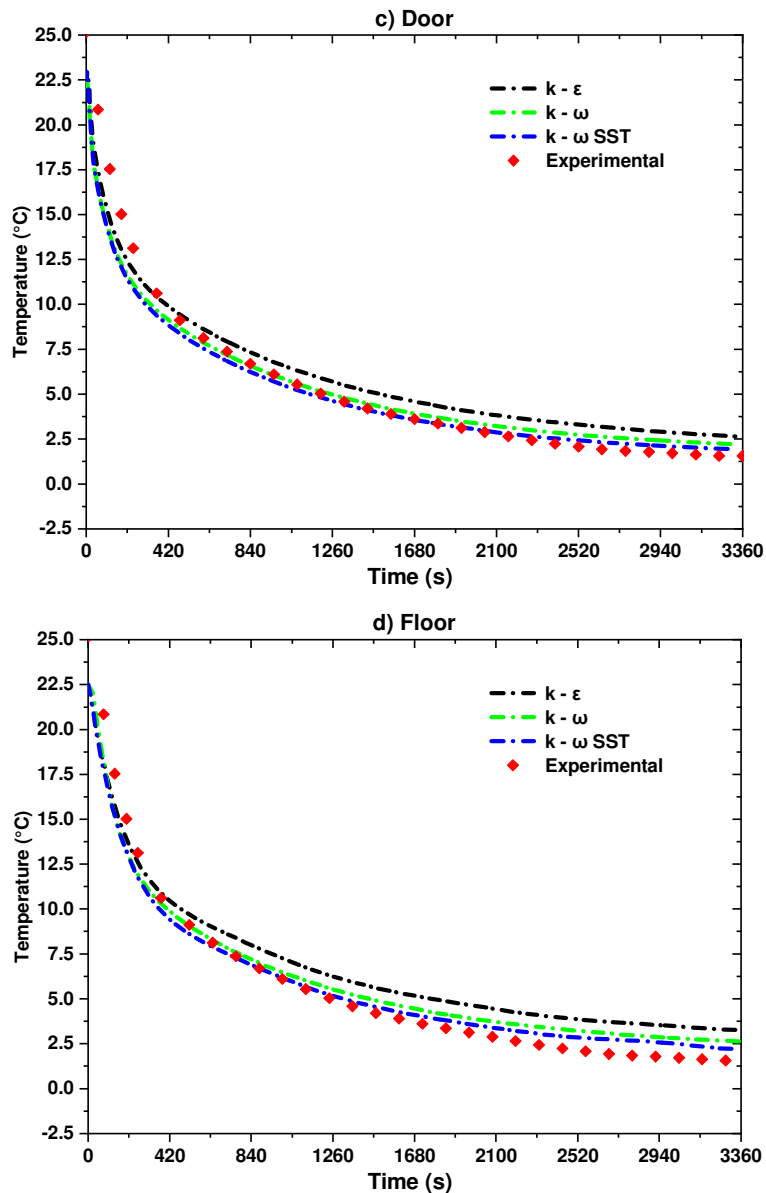


Fig. 6. Temperature values in different zones of the refrigerated truck

Therefore, the results of this study clearly demonstrate the ability of URANS turbulence models to accurately predict experimental results. To further strengthen the validity of this work, **(Table 2)** presents the root mean square error values for the three simulated turbulence models. From this table, it is obvious that the RMSE values obtained with the $k-\omega$ SST model showed better agreement with the experimental results, making this model highly favorable. That's justified by the fact that this model combines both models ($k-\omega$ and $k-\epsilon$) to accurately estimate the areas near and far from the walls. The previous results also show that the $k-\omega$ model gives acceptable results, although the inability of the $k-\epsilon$ model to also predict the thermal behavior as compared to the other models.

Table 2

RMSE values for three simulated models in the different points of analysis.

	RMSE k- ω -SST	RMSE k- ω	RMSE k- ϵ
Inlet	0,286 °C	0,299 °C	0,492 °C
Outlet	0,798 °C	0,804 °C	1,517 °C
Floor	0,914 °C	1,071 °C	1,586 °C
Door	1,222 °C	1,224 °C	1,283 °C
Global	0,805 °C	0,849 °C	1,219 °C

4.1.2. Heat Transfer and Airflow Flow Characteristics

After validation, the CFD SST k- ω model was used to obtain detailed quantitative data to characterize the aerothermal performance. In order to better understand this behavior, the following median plane represents the temperature distribution for different times [Fig.7]. At the initial moment, the temperature was about 22°C. During cooling, the coldest area is at roof level, while it increases in the rest of the truck. When the 3360s are completed, a steady-state operation is almost reached in all areas of the truck at a uniform temperature close to 0°C.

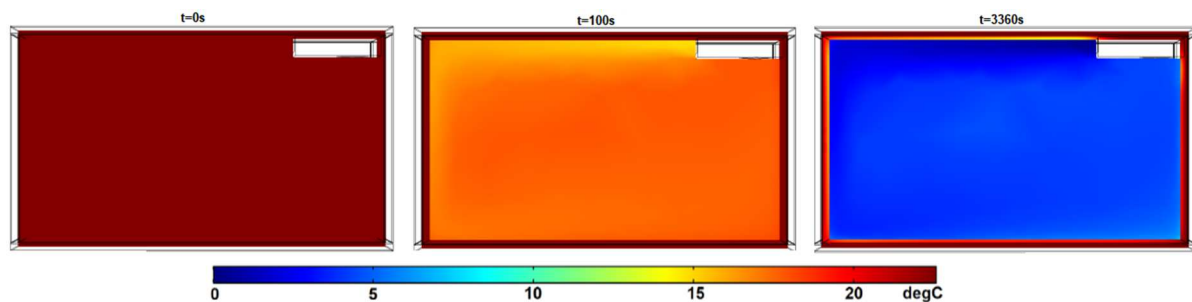


Fig. 7. Temperature distribution profiles on the plane during cooling

The cooling air enters horizontally with a velocity of 3 m/s according to the velocity component U_y . Within the parameters studied, [Fig.8] presents the speed magnitudes for different regions of the truck ($Y=1\text{m}$, 2m , 3m) on the vertical plane (Z axis) taken at the axial symmetry of the container. Near to the jet area ($Y = 1\text{m}$), the airflow clings at the roof over which it flows (Coanda effect). In the middle of the truck ($Y = 2\text{m}$), the airflow was higher near the ground, lower in the lower region, due to density and gravity. Near the door ($Y = 3\text{m}$), it is clear that the magnitude of the air speed was the lowest. Indeed, the speed decreased from 3 m / s at the air inlet level to 0.5 m / s at the rear of the truck.

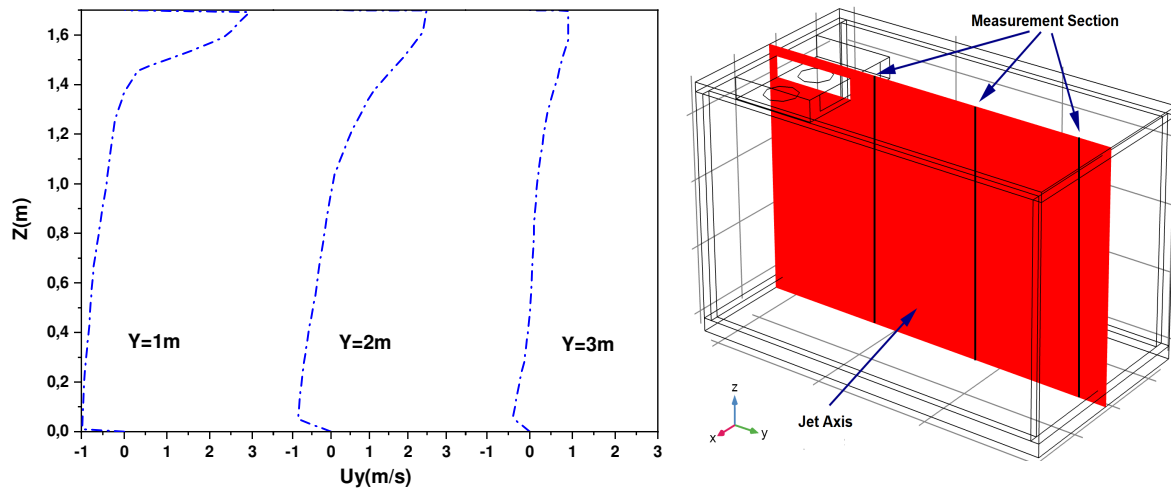


Fig. 8. Lengthwise variation of velocity profiles at XY symmetry plane

The current model was also used to determine the simulated average convective heat losses, by solving the energy equation through the envelope in contact with the outside air (left & right walls, door, front, floor and roof) [Fig.9]. The influence of insulation in the walls is observed by this quantitative study [Fig.10].

It is clear that the loss through the floor is low compared to other walls, mainly because it is the most insulated. At the roof level, it is characterized by a high air flow compared to other areas because it is close to the air jet, which leads to higher heat losses. However, the heat flow increases as the cooling period increases.

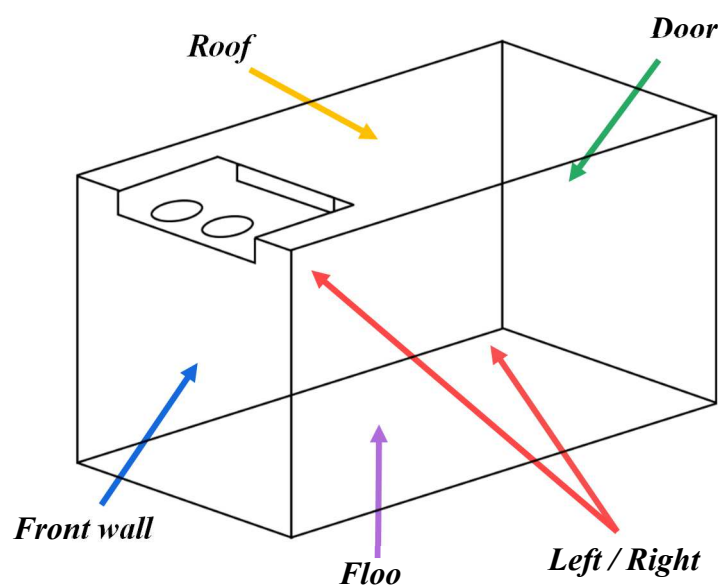


Fig. 9. Truck exterior envelope

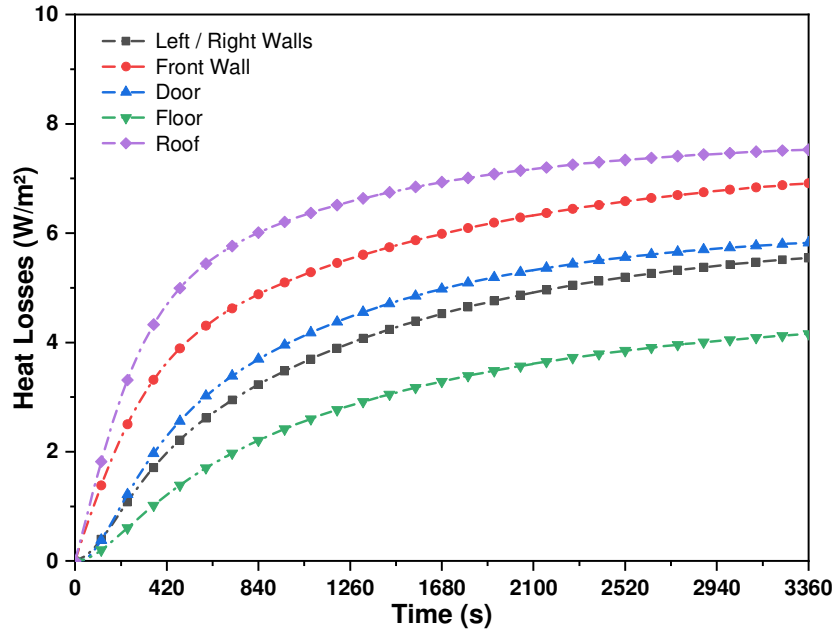


Fig. 10. Evolution of the averaged heat losses through different zones

4.1.3. Effect of Reynolds Number

In order to better understand the aerothermal characteristics in a truck, [Fig.11] illustrates the effect of Reynolds number on temperature variation during transport. This number is characterized by the hydraulic diameter of the jet section, the velocity and the kinematic viscosity. As shown in the following results, the Reynolds number of inlet flow varies in the range of 15000 to 70000. It is clear that at high numbers, the distribution of the cold temperature is improved.

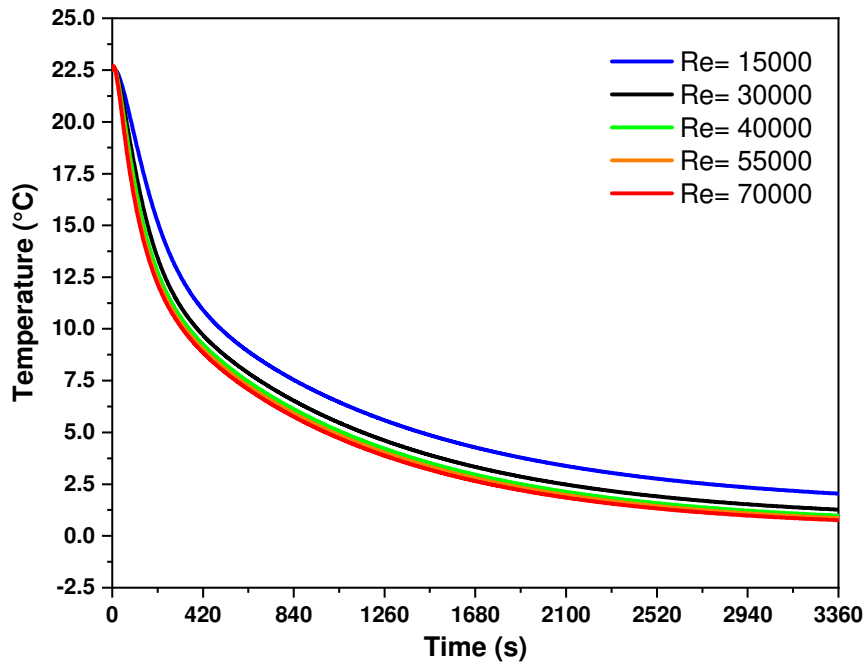


Fig. 11. Effect of Reynolds numbers on internal temperature

Referring to the obtained results [Fig.11], it can be seen that the increase in the Reynolds number has a slight impact on the time required to reduce the average air temperature in the truck from 22.5°C to 1°C. It is interesting to emphasize that the increase in the number of Reynolds leads to an increase in the ventilator power and also the cooling capacity. This allows to conclude that there is an optimal Reynolds number that can be chosen to optimize the refrigeration system in the truck.

4.2 Open Door refrigerated truck

The second part of this study aims to provide elements to explain and quantify the effect of the interaction between forced convection and natural convection, in order to obtain better control of the internal temperature for an open door refrigerated truck. This part will be divided into two sections:

- The first allows to study the effect of natural convection through an unprotected door.
- The second adopts the use of air curtain device, as an alternative solution to reduce warm air infiltration during unloading.

4.2.1. Influence of natural convection

As mentioned before, a numerical study has been developed to deal with air infiltration when opening the truck door. [Fig.12] illustrates the variation of the predicted temperature field, according to the symmetry plane of the truck.

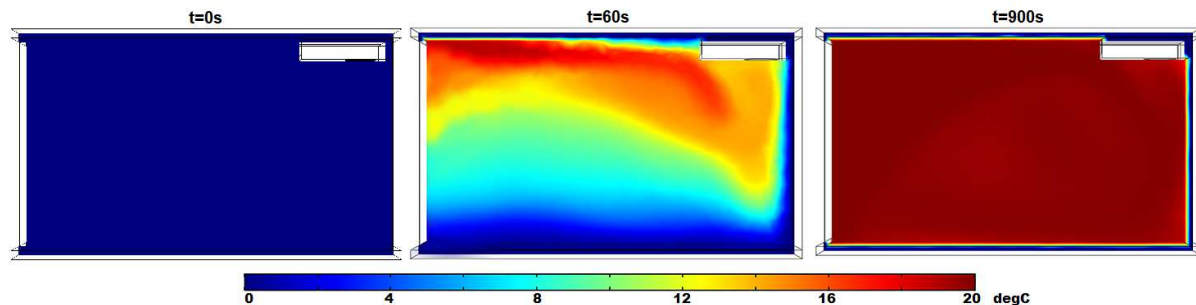


Fig. 12. Evolution of the air temperature in the opening-door geometry at different times.

After one minute of opening ($t = 60\text{s}$), it is observed that the majority of the air in the box has been renewed and the temperature begins to rise. At the floor level, the temperature variation almost remains stable. At ($t = 900\text{ s}$), the temperature profile is almost stationary with an average value of 20°C . The results show that when the door is opened, the air volume gradually heats up, from where the hot air escapes along the top of the box and the cold air exits outwards at the bottom until that the inside air is renewed. Furthermore, this heating is due to the sensible thermal load exchanged with the outside (exchange between warm and cold air) and natural convection through the open door.

In this work, a comparison between two open door scenarios (fully open and semi-open) was carried out, examining the variation in temperature during unloading. From the moment the door is open, the rate of heat through the door increases rapidly. However, as the temperature difference with the outside decreases, the internal temperature becomes almost stable.

The results show that with a full and half door opening, the temperature rises from 0°C to 19.87°C and 14.2°C after 15 min, respectively [Fig.13]. This indicates that leaving the door half open has less influence on the stability of the internal temperature than leaving the door fully open.

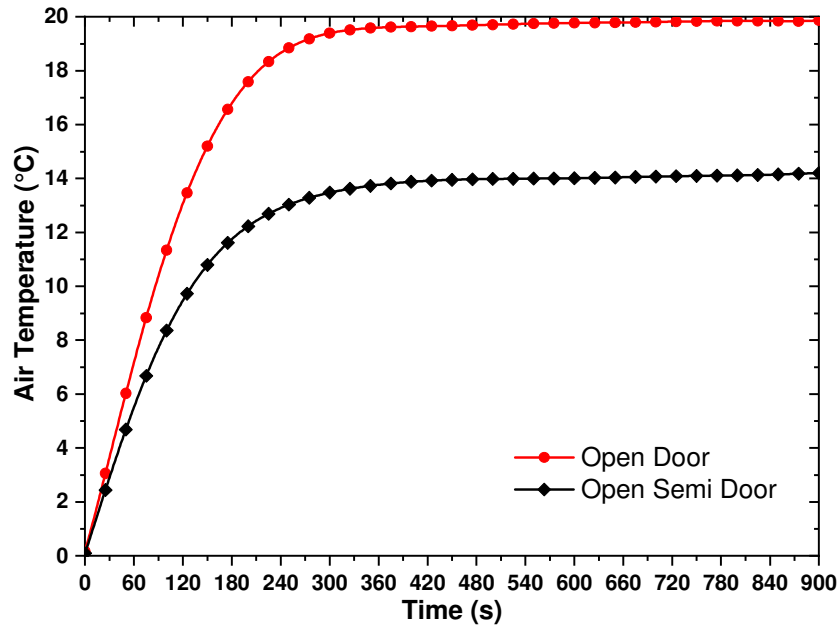


Fig. 13. Average temperature of internal air under two open door scenarios

4.2.2. Influence of air curtain

The truck door must remain open during loading or unloading. Air infiltration during these periods significantly increases the consumption of cooling energy. In order to minimize this consumption, temperature-controlled openings can lead to a significant gain, an air curtain installed near the door can be used. Furthermore, in this study, the interaction between natural convection during door opening and forced convection due to the vertical curtain jet was taken into account.

As can be seen in [Fig.14], due to the forced air flow from the air curtain, the internal temperature distribution at the bottom is higher than that at the top close to the opened door, which indicates a significant forced infiltration of air at the bottom, preventing the natural infiltration of air. Besides that, the temperature of the upper part in the rest of the truck is higher than that in the bottom part.

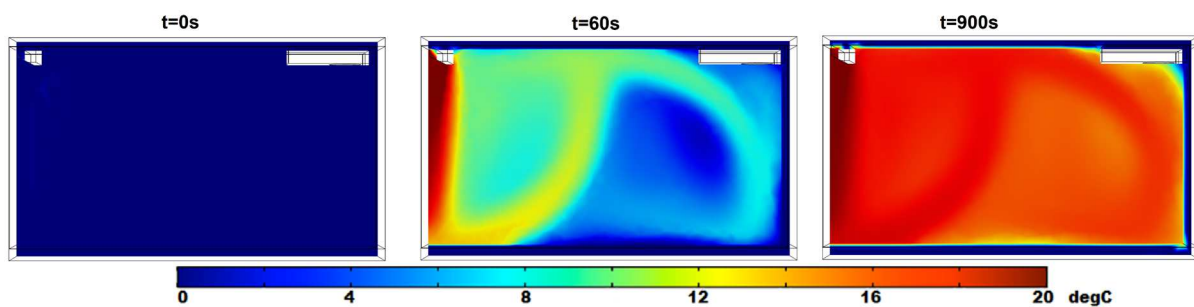


Fig. 14. Mid-plane view of the internal temperature distribution with air curtain velocity

Comparing the results of the model with and without air curtains [Fig.15], it is very easy to notice that the internal temperature values using the curtain are lower than those without protection. The temperature rise is higher than without the air curtain during the first minute. This is due to curtain instability in the initial phase of operation. After one minute, the temperature increase slows down to various degrees compared to the values obtained without the curtain.

Therefore, it can be deduced that the air curtain is capable of creating an artificial barrier (forced convection) that confines the internal air (average internal temperature decreases from 17.55°C to 12.45°C), and reduces air infiltration; this leads to reduced cooling energy consumption.

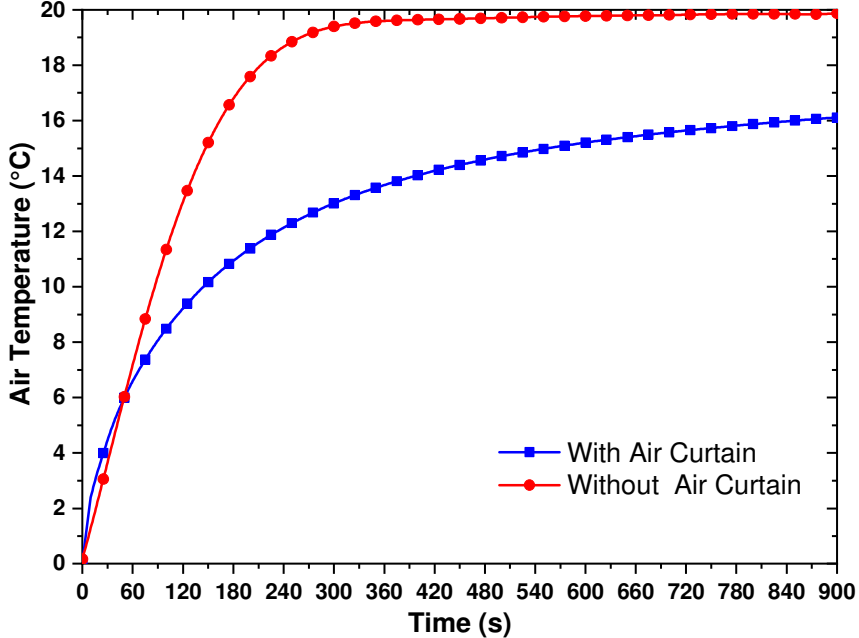


Fig. 15. Evolution of internal air temperature with and without air curtain

The following [Fig.16] illustrate the impact of loading goods into trucks to reflect a real situation with different fill rates (FR) for a door opening time of 15 minutes. It is clear that when using an air curtain, the good's average temperature is significantly lower than without an air curtain for all scenarios (FR=25%, FR=50% and FR=75%). Therefore, as the discharge rate decreases, the volume and heat capacity of the goods will reduce, resulting in an increased foodstuff temperature.

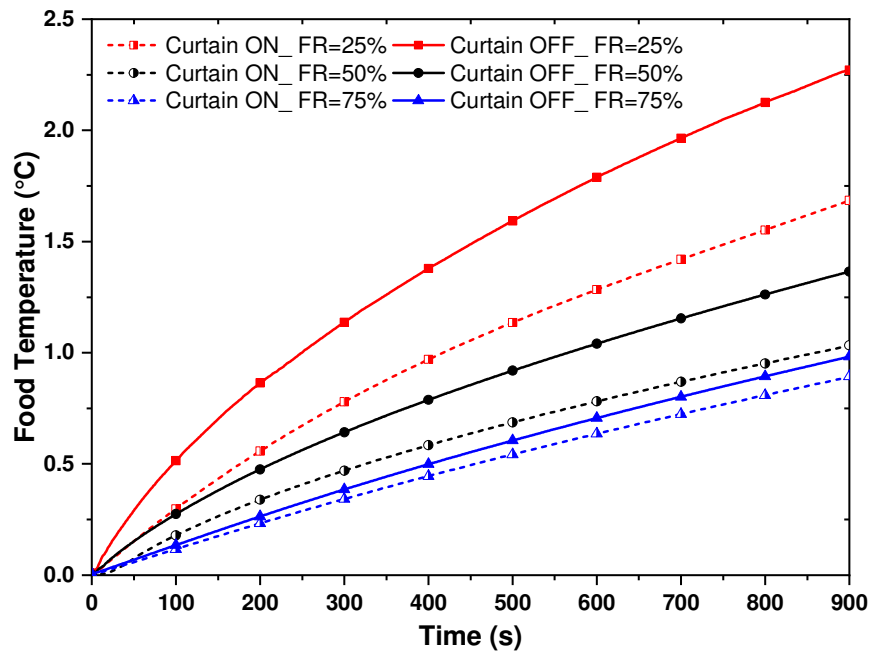


Fig. 16. Evolution of goods temperature with and without air curtain for different fill rates

4.2.3. Energy performance with and without air curtain

The following section deals with the energy performance of the refrigerated truck. Besides, the recovery energy used in this study is considered to be the energy required to bring the truck's internal and good's temperature to their set temperature. The results obtained (**Table 3**) [**Fig.17**] represent the recovery energy with and without air curtains. It is clear that using a curtain reduces this energy from 0.19 MJ, 0.68 MJ, 0.72 MJ and 0.76 MJ to 0.14 MJ, 0.54 MJ, 0.58 MJ and 0.63 MJ for the empty truck open, partially (FR = 25%), half (FR = 50%) and almost completely loading (FR = 75%), respectively. These results also indicate that the use of this device can save from 16.5% to 25.3% of the refrigeration consumption depending on the filling rate of the truck. Therefore, it is clear to see the importance of the air curtain in a refrigerated truck as an alternative solution to reduce refrigeration consumption.

Table 3
Energy efficiency using an air curtain

Geometry	Empty truck	FR=25%	FR=50%	FR=75%
Energy efficiency	25.36 %	20.75%	19.56%	16.50%

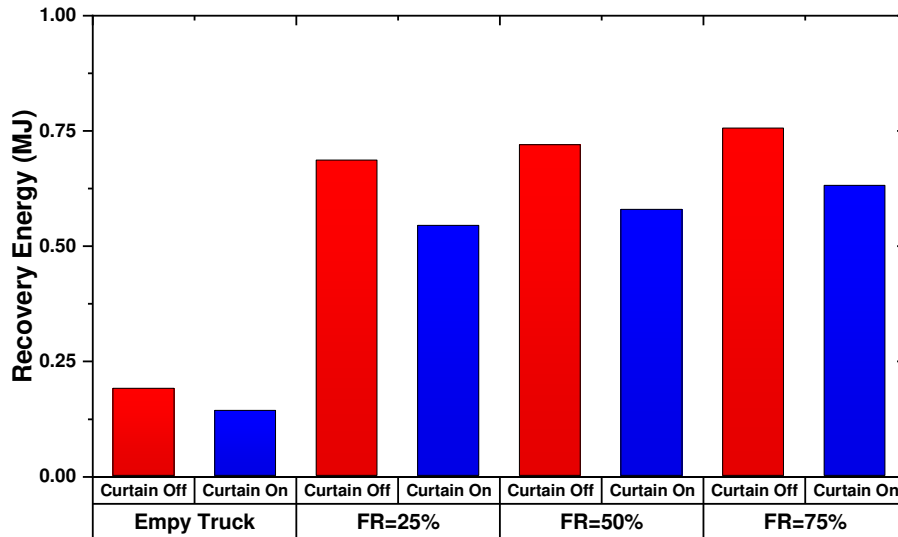


Fig. 17. Recovery energy during the loading of refrigerated truck

5. Conclusion

Refrigerated truck transport directly affects the quality and shelf life of specialized perishable products, which are key elements in the cold chain. In this context, it is important to examine the cooling mechanism to improve and optimize the energy efficiency inside a refrigerated truck. However, this study was conducted to gain knowledge on aerothermal behavior and to understand the flow mechanisms in various three-dimensional configurations of a refrigerated truck and to complement previous studies on conjugate heat transfer.

Different URANS unsteady turbulence models (standard $\kappa\text{-}\omega$, SST $\kappa\text{-}\omega$, standard $\kappa\text{-}\epsilon$) in a closed-door refrigerated truck were discussed. The results showed that there was no significant difference between the different turbulence models and the measured temperatures. The RMSE values obtained with the SST $\kappa\text{-}\omega$ model had a better agreement, which makes this model very favorable.

The quantitative and qualitative investigation in the truck examined showed the influence of insulation in the walls to evacuate internal heat losses, and the variation of Reynolds number on the internal thermal behavior to stretch the applicability of this study.

To optimize energy consumption and cooling time, the effect of the interaction between natural and forced convection on the cooling capacity when opening the door, was taken into account by using an air curtain. However, this curtain is capable of creating an artificial barrier that confines the internal air, and reduces air infiltration when the door is opened.

In order to address more complex tasks related to cooling energy performance, other developments may include as perceptive of this study such as:

- Cyclic dynamic simulation of a cooling unit during the opening and closing of the truck door.
- Simulation of combined phenomena during a trip considering the internal conditions and the surrounding environment that will result in a variety of temperature and relative humidity inside the truck
- Detailed simulation of the filling effect for certain types of perishable foods.
- Simulation of latent heat incorporation using PCMs to store cold and improve refrigeration performance.

Reference

- Ashok, A., Brison, M., LeTallec, Y., 2017. Improving cold chain systems: Challenges and solutions. *Vaccine* 35, 2217–2223. <https://doi.org/10.1016/j.vaccine.2016.08.045>
- Ben Taher, M.A., Kousksou, T., Makroum, H., Ahachad, M., Mahdaoui, M., 2020. Numerical Study of a Non-isothermal Refrigerated Truck. *Adv. Intell. Syst. Comput.* https://doi.org/10.1007/978-3-030-36671-1_43
- BIS Research, 2019. Global Food Cold Chain Market: Focus on Type (Refrigerated Storage and Refrigerated Transportation), Temperature Type (Chilled and Frozen), and Application - Analysis and Forecast, 2019-2024.
- Brightec, 2020. Brightec Bright Blue Company [WWW Document]. URL <https://www.brightec.nl> (accessed 5.2.20).
- COMSOL, 2020. Comsol Multiphysics. COMSOL AB, Stock. Sweden.
- Cong, L., Yu, Q., Qiao, G., Li, Y., Ding, Y., 2019. Effects of an Air Curtain on the Temperature Distribution in Refrigerated Vehicles under a Hot Climate Condition. *J. Therm. Sci. Eng. Appl.* 11, 1–30. <https://doi.org/10.1115/1.4043467>
- de Palma, A., Lindsey, R., Quinet, E., Vickerman, R., 2011. A handbook of transport economics, A Handbook of Transport Economics. <https://doi.org/10.4337/9780857930873>
- Getahun, S., Ambaw, A., Delele, M., Meyer, C.J., Opara, U.L., 2017. Analysis of airflow and heat transfer inside fruit packed refrigerated shipping container: Part I – Model development and validation. *J. Food Eng.* 203, 58–68. <https://doi.org/10.1016/j.jfoodeng.2017.02.010>
- Han, J.-W., Zhu, W.-Y., Ji, Z.-T., 2019. Comparison of veracity and application of different CFD turbulence models for refrigerated transport. *Artif. Intell. Agric.* 3, 11–17. <https://doi.org/10.1016/j.aiia.2019.10.001>
- Hoang, M.H., Laguerre, O., Moureh, J., Flick, D., 2012. Heat transfer modelling in a ventilated cavity loaded with food product: Application to a refrigerated vehicle. *J. Food Eng.* 113, 389–398. <https://doi.org/10.1016/j.jfoodeng.2012.06.020>
- James, S.J., James, C., 2010. The food cold-chain and climate change. *Food Res. Int.* 43,

- 1944–1956. <https://doi.org/10.1016/j.foodres.2010.02.001>
- Jara, P.B.T., Rivera, J.J.A., Merino, C.E.B., Silva, E.V., Farfán, G.A., 2019. Thermal behavior of a refrigerated vehicle: Process simulation. *Int. J. Refrig.* 100, 124–130. <https://doi.org/10.1016/j.ijrefrig.2018.12.013>
- Jiang, T., Xu, N., Luo, B., Deng, L., Wang, S., Gao, Q., Zhang, Y., 2020. Analysis of an internal structure for refrigerated container: Improving distribution of cooling capacity. *Int. J. Refrig.* 113, 228–238. <https://doi.org/10.1016/j.ijrefrig.2020.01.023>
- Jones, W., Launder, B., 1972. The prediction of laminarization with a two-equation model of turbulence. *Int. J. Heat Mass Transf.* 15, 301–314. [https://doi.org/10.1016/0017-9310\(72\)90076-2](https://doi.org/10.1016/0017-9310(72)90076-2)
- Kayfeci, M., Keçebaş, A., Gedik, E., 2013. Determination of optimum insulation thickness of external walls with two different methods in cooling applications. *Appl. Therm. Eng.* 50, 217–224. <https://doi.org/10.1016/j.applthermaleng.2012.06.031>
- Lafaye De Micheaux, T., Ducoulombier, M., Moureh, J., Sartre, V., Bonjour, J., 2015. Experimental and numerical investigation of the infiltration heat load during the opening of a refrigerated truck body. *Int. J. Refrig.* 54, 170–189. <https://doi.org/10.1016/j.ijrefrig.2015.02.009>
- Menter, F.R., 1994. Two-equation eddy-viscosity turbulence models for engineering applications. *AIAA J.* 32, 1598–1605. <https://doi.org/10.2514/3.12149>
- Merai, M., Duret, S., Derens, E., Leroux, A., Flick, D., Laguerre, O., 2019a. Experimental characterization and modelling of refrigeration of pork carcasses during transport under field conditions. *Int. J. Refrig.* 102, 77–85. <https://doi.org/10.1016/j.ijrefrig.2019.02.033>
- Merai, M., Flick, D., Guillier, L., Duret, S., Laguerre, O., 2019b. Experimental characterization of heat transfer inside a refrigerated trailer loaded with carcasses. *Int. J. Refrig.* 99, 194–203. <https://doi.org/10.1016/j.ijrefrig.2018.11.041>
- Moureh, J., Menia, N., Flick, D., 2002. Numerical and experimental study of airflow in a typical refrigerated truck configuration loaded with pallets. *Comput. Electron. Agric.* 34, 25–42. [https://doi.org/10.1016/S0168-1699\(01\)00178-8](https://doi.org/10.1016/S0168-1699(01)00178-8)
- Moureh, J., Tapsoba, S., Derens, E., Flick, D., 2009. Air velocity characteristics within vented pallets loaded in a refrigerated vehicle with and without air ducts. *Int. J. Refrig.* 32, 220–

234. <https://doi.org/10.1016/j.ijrefrig.2008.06.006>
- O'Sullivan, J., Ferrua, M., Love, R., Verboven, P., Nicolaï, B., East, A., 2014. Airflow measurement techniques for the improvement of forced-air cooling, refrigeration and drying operations. *J. Food Eng.* 143, 90–101. <https://doi.org/10.1016/j.jfoodeng.2014.06.041>
- Oltersdorf, U., 2003. Developments in food processing and increasing gaps in consumers competence of food handling—the challenge for nutrition policy in Europe. *J. Food Eng.* 56, 163–169. [https://doi.org/10.1016/S0260-8774\(02\)00245-5](https://doi.org/10.1016/S0260-8774(02)00245-5)
- Oró, E., Miró, L., Farid, M.M., Cabeza, L.F., 2012. Improving thermal performance of freezers using phase change materials. *Int. J. Refrig.* 35, 984–991. <https://doi.org/10.1016/j.ijrefrig.2012.01.004>
- Panozzo, G., Minotto, G., Barizza, A., 1999. Transport et distribution de produits alimentaires. *Int. J. Refrig.* 22, 625–639. [https://doi.org/10.1016/S0140-7007\(99\)00023-7](https://doi.org/10.1016/S0140-7007(99)00023-7)
- Rai, A., Sun, J., Tassou, S.A., 2019. Numerical investigation of the protective mechanisms of air curtain in a refrigerated truck during door openings. *Energy Procedia* 161, 216–223. <https://doi.org/10.1016/j.egypro.2019.02.084>
- Saguy, I.S., Singh, R.P., Johnson, T., Fryer, P.J., Sastry, S.K., 2013. Challenges facing food engineering. *J. Food Eng.* 119, 332–342. <https://doi.org/10.1016/j.jfoodeng.2013.05.031>
- Senguttuvan, S., Youn, J.-S., Park, J., Lee, J., Kim, S.-M., 2020. Enhanced airflow in a refrigerated container by improving the refrigeration unit design. *Int. J. Refrig.* <https://doi.org/10.1016/j.ijrefrig.2020.08.019>
- Sirén, K., 2003. Technical dimensioning of a vertically upwards-blowing air curtain - Part II. *Energy Build.* 35, 697–705. [https://doi.org/10.1016/S0378-7788\(02\)00224-4](https://doi.org/10.1016/S0378-7788(02)00224-4)
- Tanner, D., 2016. Refrigerated Transport, in: Reference Module in Food Science. Elsevier. <https://doi.org/10.1016/B978-0-08-100596-5.03485-5>
- Tso, C.P., Yu, S.C.M., Poh, H.J., Jolly, P.G., 2002. Experimental study on the heat and mass transfer characteristics in a refrigerated truck. *Int. J. Refrig.* 25, 340–350. [https://doi.org/10.1016/S0140-7007\(01\)00015-9](https://doi.org/10.1016/S0140-7007(01)00015-9)
- Verdouw, C.N., Wolfert, J., Beulens, A.J.M., Rialland, A., 2016. Virtualization of food

supply chains with the internet of things. *J. Food Eng.* 176, 128–136. <https://doi.org/10.1016/j.jfoodeng.2015.11.009>

Wilcox, D.C., 2006. *Turbulence Modeling for CFD (Third Edition)*. DCW Ind.

Wilcox, D.C., 1988. Reassessment of the scale-determining equation for advanced turbulence models. *AIAA J.* 26, 1299–1310. <https://doi.org/10.2514/3.10041>

Xie, Y., Brecht, J.K., Abrahan, C.E., Bornhorst, E.R., Luo, Y., Monge, A.L., Vorst, K., Brown, W., 2021. Improving temperature management and retaining quality of fresh-cut leafy greens by retrofitting open refrigerated retail display cases with doors. *J. Food Eng.* 292, 110271. <https://doi.org/10.1016/j.jfoodeng.2020.110271>

Zhang, X., Han, J.W., Qian, J.P., Wang, Y.Z., Wang, L., Yang, X.T., 2018. Computational fluid dynamic study of thermal effects of open doors of refrigerated vehicles. *J. Food Process Eng.* 41, 1–13. <https://doi.org/10.1111/jfpe.12662>